

Effects of Stuffer DNA on the Suppression of Choroidal Neovascularization by a rAAV Expressing a mTOR-Inhibiting shRNA

Steven Hyun Seung Lee,^{1,2,9} HeeSoon Chang,^{3,9} Hee Jong Kim,³ Jun-Sub Choi,³ Jin Kim,³ Ji Hyun Kim,^{1,2} Ha-Na Woo,^{1,2} Seung Kwan Nah,⁴ Sang Joon Jung,⁴ Joo Yong Lee,^{2,5,6} Keerang Park,⁷ Tae Kwann Park,^{4,8} and Heuiran Lee^{1,2}

¹Department of Microbiology, College of Medicine, University of Ulsan, Seoul 05505, Korea; ²Bio-Medical Institute of Technology, College of Medicine, University of Ulsan, Seoul 05505, Korea; ³CuroGene Life Sciences Co., Ltd., Cheongju 28578, Korea; ⁴Department of Ophthalmology, Soonchunhyang University Hospital Bucheon, Bucheon 14584, Korea; ⁵Department of Ophthalmology, University of Ulsan, College of Medicine, Seoul 05505, Korea; ⁶Asan Medical Center, University of Ulsan, College of Medicine, Seoul 05505, Korea; ⁷Department of Biopharmacy, Chungbuk Health & Science University, Cheongju 28150, Korea; ⁸Department of Ophthalmology, College of Medicine, Soonchunhyang University, Cheonan 31151, Korea

Choroidal neovascularization (CNV) is the defining characteristic of the wet subtype of age-related macular degeneration (AMD), which is a rapidly growing global health problem. Previously, we had demonstrated the therapeutic potential of gene therapy against CNV using short hairpin RNA (shRNA) delivered via recombinant adeno-associated virus (rAAV), which abrogates mammalian-to-mechanistic (mTOR) activity in a novel manner by simultaneously inhibiting both mTOR complexes. Both the target and use of gene therapy represent a novel treatment modality against AMD. Here, the xenogeneic GFP gene used as a reporter in previous studies was removed from the virus vector to further develop the therapeutic for clinical trials. Instead, a stuffer DNA derived from the 3' UTR of the human UBE3A gene was used to ensure optimal viral genome size for efficient rAAV assembly. The virus vector containing the stuffer DNA, rAAV2-shmTOR-SD, positively compares to one encoding the shRNA and a GFP expression cassette in terms of reducing CNV in a laser-induced mouse model, as determined by fundus fluorescein angiography. These results were confirmed via immunohistochemistry using anti-CD31, while a TUNEL assay showed that rAAV2-shmTOR-SD possesses anti-apoptotic properties as well. The qualities exhibited by rAAV2-shmTOR-SD demonstrate its potential as a human gene therapeutic for the treatment of wet AMD.

INTRODUCTION

Age-related macular degeneration (AMD) is the leading cause of blindness in the elderly population of developed nations,¹ and it can be divided into two major subtypes: dry AMD is marked by geographic atrophy, whereas choroidal neovascularization characterizes wet AMD.² The most common treatment strategy against wet AMD involves inhibiting vascular endothelial growth factor (VEGF) via intravitreal injections given every 4–8 weeks, depending on the therapeutic. Among anti-VEGF drugs, ranibizumab and

afibercept are US Food and Drug Administration (FDA) approved, while bevacizumab is popularly used off-label due to its economic advantages. The need for the frequent administration of injection-based wet AMD treatments makes it economically and procedurally burdensome, negatively affecting patient compliance.³ As wet AMD is a progressive, degenerative disease,² negative patient compliance significantly threatens treatment outcomes,⁴ illustrating the limitations of current therapeutics. Furthermore, previous studies have shown that sustained VEGF suppression may have adverse effects on the retina,^{5,6} raising further questions about the viability of conventional anti-VEGF therapies. With AMD projected to affect approximately 288 million patients by 2040,¹ the development of a gene therapeutic focused on a different target may prove a necessary and beneficial alternative approach to this growing global health concern.

Recently, we have described the effects of recombinant adeno-associated virus (rAAV)-mammalian-to-mechanistic (mTOR) short hairpin RNA (shRNA), an shRNA targeting mTOR packaged in rAAV2, in a laser-induced choroidal neovascularization (CNV) mouse model. Here renamed rAAV2-shmTOR-GFP, the virus vector was shown to effectively transduce mouse retinas and effect its anti-angiogenic and anti-inflammatory properties,⁷ thereby addressing some of the major symptoms of wet AMD.

Received 26 February 2019; accepted 21 June 2019;
<https://doi.org/10.1016/j.omtm.2019.06.004>.

⁹These authors contributed equally to this work.

Correspondence: Heuiran Lee, PhD, Department of Microbiology and Bio-Medical Institute of Technology, College of Medicine, University of Ulsan, 88 Olympic-ro 43-gil Songpa-gu, Seoul 05505, Korea.
E-mail: heuiran@amc.seoul.kr

Correspondence: Tae Kwann Park, MD, PhD, Department of Ophthalmology, Soonchunhyang University Hospital Bucheon, 170, Jomaru-ro, Wonmi-gu, Bucheon 14584, Korea.
E-mail: tkpark@schmc.ac.kr



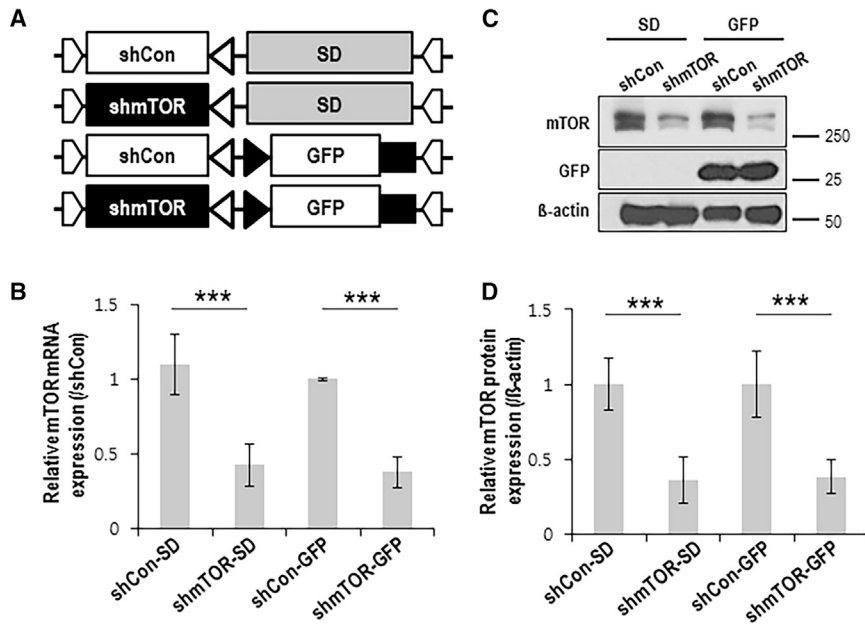


Figure 1. Characterization of rAAV2-shmTOR-SD *In Vitro*

Schematic representation of the various virus vectors (A). The entire GFP expression cassette of rAAV2-shmTOR-GFP has been replaced with a stuffer DNA derived from the 3' UTR of the human UBE3A gene to produce rAAV2-shmTOR-SD. Normalized relative to mock-treated ARPE-19 cells, quantitative analysis conducted via qRT-PCR showed that both the GFP- and stuffer DNA-containing virus vectors yielded significantly reduced mTOR mRNA expression when compared to their counterparts containing a control shRNA (B). At 48 h after treatment with the various virus vectors, mTOR expression was determined via western blotting from ARPE-19 cells (C), with β -actin used as a protein loading control, and the results were quantified thereafter (D).

Present in virtually all eukaryotic cells, mTOR is a serine-threonine kinase serving as the catalytic component of two separate complexes, mTORC1 and mTORC2. Each complex has its own attendant signaling pathway, and both interact with a variety of other.⁸ As such, mTOR is involved in a vast number of cellular processes, and its dysfunction has been implicated in a number of disease states, including ocular disorders.⁹ mTOR has subsequently been identified as a potential therapeutic target for wet AMD,¹⁰ with mTOR inhibition proven to inhibit CNV both *in vitro*¹¹ and *in vivo*,¹² though the mechanism by which this occurs has yet to be elucidated. Earliest examples of mTOR inhibition utilized rapamycin or its structural analogs, which only affect mTORC1. This was followed by a number of groups attempting to simultaneously inhibit both complexes by blocking the phosphorylation of the downstream targets of mTORC1 and mTORC2.¹³ In contrast, we used a program developed in-house called CAPSID (Convenient Application Program for siRNA Design) to design a novel small interfering RNA (siRNA) that directly downregulates mTOR, resulting in the inhibition of both mTOR complexes.^{14,15}

Adeno-associated viruses are well suited for gene therapy applications because they are non-pathogenic in nature, transduce in dividing and non-dividing cells, and have the ability for long-term transgene expression.¹⁶ This was confirmed in late 2017 when the FDA approved voretigene neparvovec-rzyl (Luxturna), which uses an rAAV2 to deliver a human retinal pigment epithelium (RPE)65 cDNA to treat Leber's congenital amaurosis resulting from a mutation in the RPE65 gene.¹⁷ Additional studies have shown that retinal inflammation or a pathological state may actually enhance rAAV transduction,^{18,19} which is especially relevant for wet AMD gene therapeutics. rAAV2-shmTOR-GFP carried a GFP reporter gene in earlier studies,⁷ but GFP's connections with cytotoxicity and immune responses²⁰ make its inclusion deleterious for a human gene

therapeutic; the xenogeneic transgene has been removed and replaced with a stuffer DNA. We report here that the resulting virus vector, rAAV2-shmTOR-stuffer DNA (SD), was able to directly inhibit mTOR and was as efficacious *in vivo* as rAAV2-shmTOR-GFP in addressing CNV, the major characteristic of wet AMD. Furthermore, rAAV2-shmTOR-SD was shown to possess anti-apoptotic capabilities, once again demonstrating its suitability as a wet AMD gene therapeutic.

RESULTS

In Vitro Efficacy of rAAV2-shmTOR-SD

mTOR inhibition in cells treated with the virus vectors was measured via qRT-PCR and western blotting (Figure 1A). rAAV2-shmTOR-GFP (0.38 ± 0.10 , $p < 0.001$) and rAAV2-shmTOR-SD (0.43 ± 0.14 , $p < 0.001$) administration markedly reduced mTOR mRNA levels relative to rAAV2-shCon (control shRNA)-GFP (Figure 1B). Western blotting confirmed that the virus vectors delivering the mTOR-inhibiting shRNA elicited significantly lower amounts of mTOR when compared to their counterparts containing control shRNA and that those containing the SD in place of the GFP transgene did not express GFP (Figure 1C). Quantification of the latter yielded mTOR protein levels of 1.00 ± 0.17 , 1.00 ± 0.22 , 0.36 ± 0.16 ($p < 0.001$), and 0.38 ± 0.11 ($p < 0.001$) for rAAV2-shCon-SD, rAAV2-shCon-GFP, rAAV2-shmTOR-SD, and rAAV2-shmTOR-GFP, respectively, relative to β -actin, used here as a protein loading control (Figure 1D).

In Vivo Efficacy of rAAV2-shmTOR-SD

Western blotting was used to resolve proteins isolated from the retinas of the laser-induced CNV mouse model to demonstrate the *in vivo* activity of rAAV2-shmTOR-SD (Figure 2A). Compared to the control group (2.63 ± 0.26) and those administered rAAV2-shCon-SD (2.16 ± 0.35), rAAV2-shmTOR-SD treatment resulted in markedly reduced mTOR expression levels (1.33 ± 0.17 , $p = 0.002$) (Figure 2B). These results mirrored those obtained by immunostaining transverse retinal sections (Figure 2C). While GFP expression was absent in

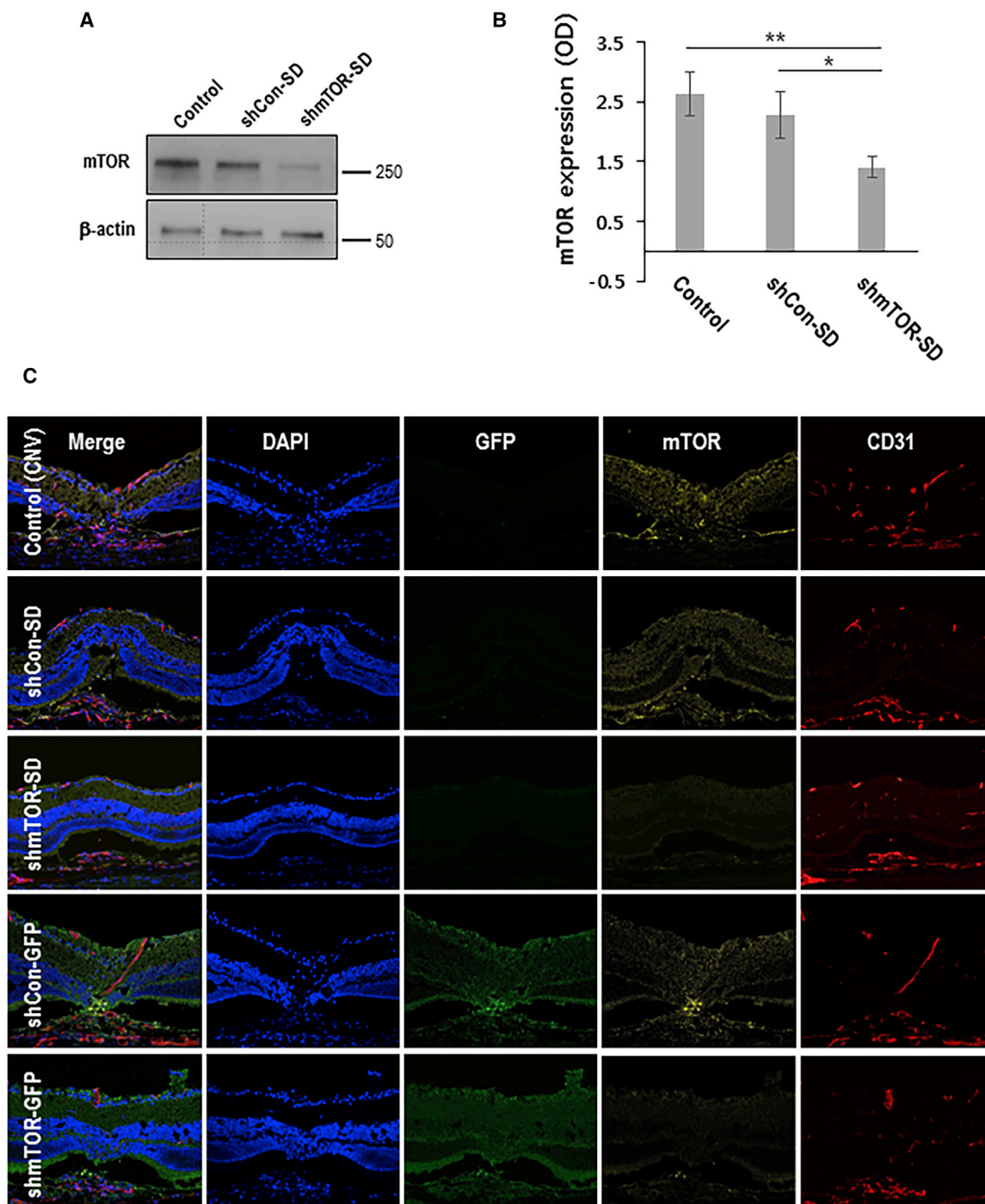


Figure 2. In Vivo Activity of rAAV2-shmTOR-SD and Retinal Transduction of the Mouse Model

Western blots of retinal tissue samples, again using β-actin as a loading control (A), demonstrated that rAAV2-shCon-SD treatment had little effect on mTOR expression, while it was significantly downregulated by rAAV2-shmTOR-SD (B) (n = 3). Immunohistochemistry performed on frozen sections showed that the various virus vectors were able to successfully transduce the retinas of the laser-induced mouse model and exert their desired effects on the target tissue (C).

samples taken from these three groups, it was detected in frozen sections prepared from mice injected with rAAV2-shCon-GFP and rAAV2-shmTOR-GFP, showing that the SD achieved its purpose.

Along with this presence of GFP, the downregulation of mTOR observed in mice treated with rAAV2-shmTOR-SD and rAAV2-shmTOR-GFP, compared to their control shRNA-containing

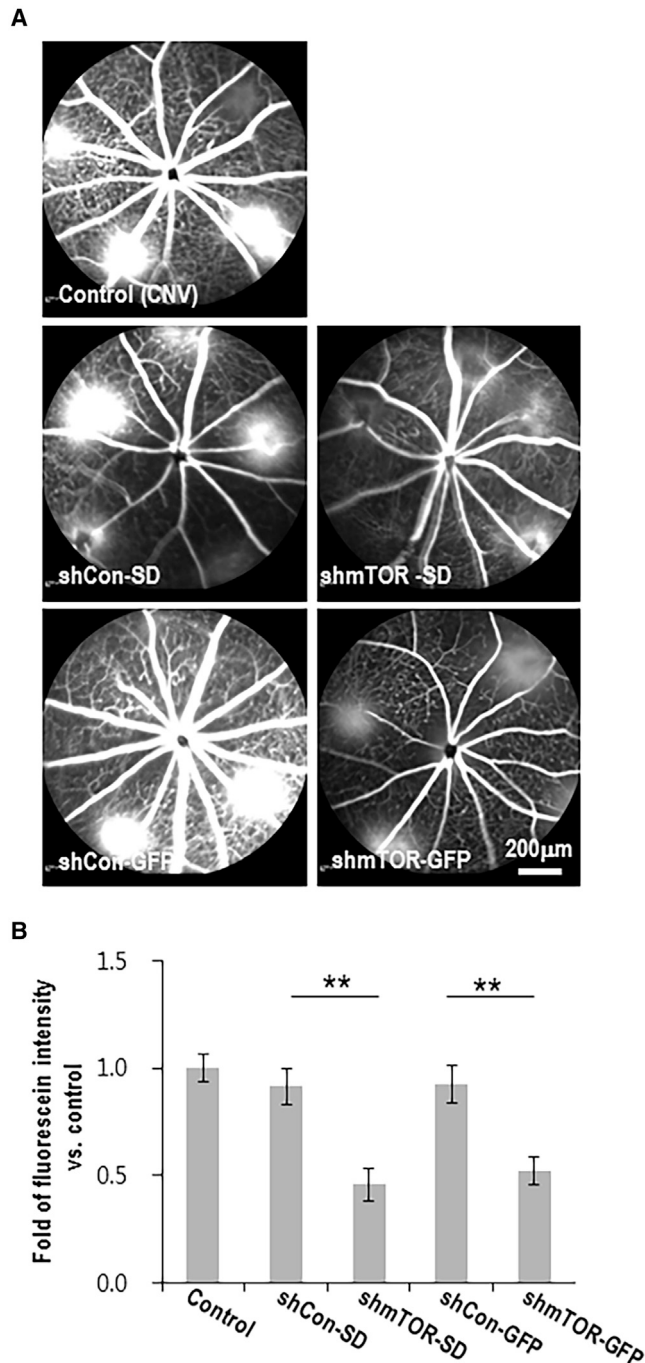


Figure 3. Fundus Fluorescein Angiography

FFA performed 1 day prior to sacrifice showed extensive new vessel development resulting from laser photocoagulation in the retinas of mock-treated mice and in those treated with control shRNA-containing virus vectors. This activity was significantly abrogated upon rAAV2-shmTOR-SD and rAAV2-shmTOR-GFP transduction (A), which was then quantified (B) ($n = 3$).

counterparts, provided further evidence of successful retinal transduction by the virus vectors.

Anti-angiogenic Activity of rAAV2-shmTOR-SD

The anti-angiogenic activity of rAAV2-shmTOR-SD resulting from mTOR inhibition was demonstrated via fundus fluorescein angiography (FFA) and immunostaining whole mounts of RPE-choroid tissue. FFA was performed 13 days post-laser photocoagulation, which confirmed the formation of new vessels in the mock-treated control group (Figure 3A). Mice treated with virus vectors containing control siRNA along with either the SD (0.92 ± 0.09) or the GFP reporter transgene expression cassette (0.93 ± 0.09) showed little difference versus the control, whereas both rAAV2-shmTOR-SD (0.46 ± 0.07 , $p = 0.0021$) and rAAV2-shmTOR-GFP (0.52 ± 0.07 , $p = 0.0026$) exhibited significantly reduced levels of new vessel formation (Figure 3B). These results were verified by immunohistochemistry performed with anti-CD31 (Figure 4A). This revealed that CNV extensiveness was reduced to 0.26 ± 0.09 ($p = 0.0036$) for mice treated with rAAV2-shmTOR-SD from 0.89 ± 0.27 for those treated with rAAV2-shCon-SD, relative to mock-treated controls. This mirrors the results obtained from virus vectors containing the GFP reporter gene, with 0.86 ± 0.20 for the control shRNA and 0.36 ± 0.11 ($p = 0.0038$) for the mTOR-inhibiting construct (Figure 4B). As can be seen, rAAV2-shmTOR-SD was as effective as rAAV2-shmTOR-GFP, the virus vector characterized in our previous study,⁷ in decreasing new vessel formation, thereby reducing CNV extensiveness.

Anti-apoptotic Effect of rAAV2-shmTOR-SD

TUNEL assays performed on transverse retinal sections confirmed the presence of apoptotic cells speckled throughout the retinas of mock-treated mice and those administered with rAAV2-shCon-SD or rAAV2-shCon-GFP, including in the outer nuclear layer, inner nuclear layer, and ganglion cell layer. On the other hand, significantly fewer were found in mice treated with virus vectors expressing the mTOR-inhibiting shRNA (Figure 5A). Relative to the mock-treated control group, rAAV2-shmTOR-SD and rAAV2-shmTOR-GFP contained 0.27 ± 0.12 ($p = 0.019$) and 0.41 ± 0.16 ($p = 0.028$) TUNEL-positive cells, respectively, as opposed to 0.97 ± 0.29 for rAAV2-shCon-SD and 1.05 ± 0.29 for rAAV2-shCon-GFP, with the decrease showing that rAAV2-shmTOR-SD, much like rAAV2-shmTOR-GFP, has anti-apoptotic activity (Figure 5B).

DISCUSSION

Here we demonstrate the ability of rAAV2-shmTOR-SD to reduce CNV through mTOR inhibition in the retinas of a laser-induced mouse model. After verifying via qRT-PCR and western blotting that its intended effects upon the target molecule were as potent as the previously characterized rAAV2-shmTOR-GFP,⁷ rAAV2-shmTOR-SD activity was further confirmed *in vivo*. When compared to both mock-treated animals and those treated with control shRNAs, rAAV2-shmTOR-SD was shown to decrease new vessel formation in the retina while also exhibiting anti-apoptotic qualities. These results mirror the effects of rAAV2-shmTOR-GFP, showing the suitability of the newly constructed virus vector as a potential wet AMD gene therapeutic and

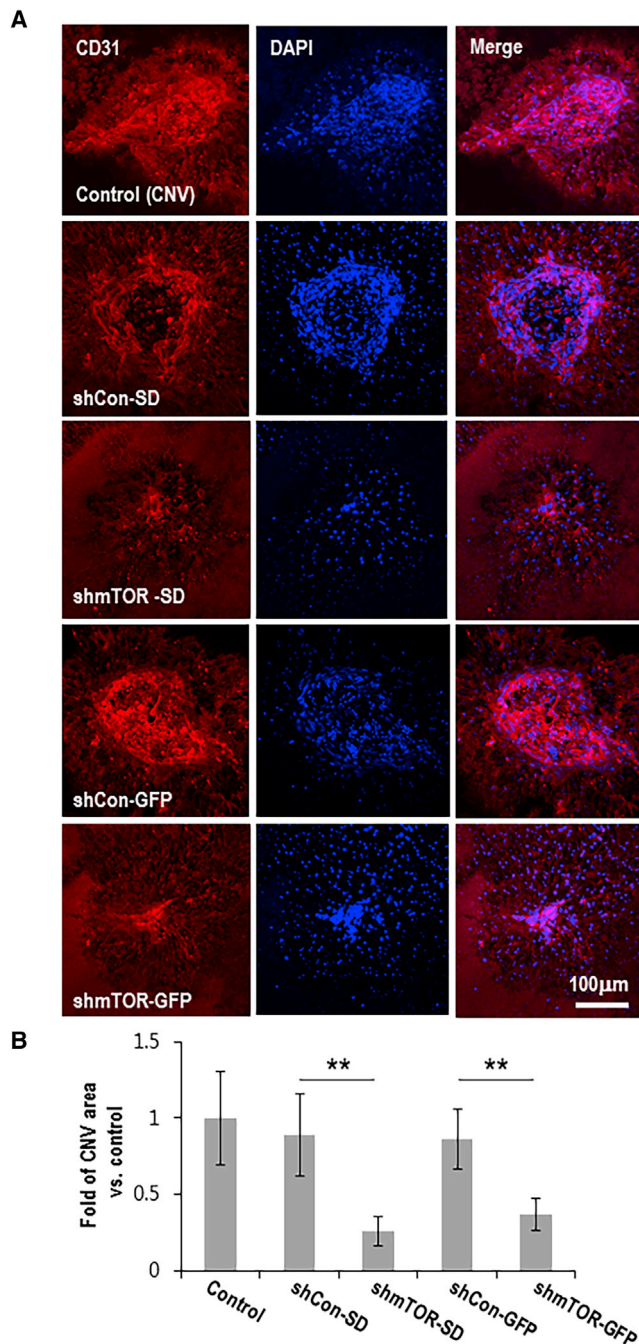


Figure 4. Visualization of CNV Extensiveness Resulting from Laser Photocoagulation

Whole-mount immunostaining using anti-CD31 to observe endothelial cells revealed that CNV was widespread in control mice and those treated with rAAV2-shCon-SD and rAAV2-shCon-GFP. In contrast, CNV extensiveness was markedly reduced in mice treated with rAAV2-shmTOR-SD and rAAV2-shmTOR-GFP (A), with the difference being especially pronounced between the virus vectors containing the stuffer DNA (B) (n = 6).

one able to overcome the shortcomings of currently employed anti-VEGF treatments.^{3–6} rAAV2-shmTOR-SD, which replaces the GFP expression cassette with a SD, is a precursor to developing wet AMD gene therapeutics that are safe, sustainable, and effective.

The FDA has set forth its recommendations regarding the expression of transgenes for human gene therapeutics in a pair of publications. Specific to retinal disorders, a draft guidance suggests considering any inflammatory or immune responses resulting from the transgene, as well as potential local and systemic toxicities.²¹ Additionally, expression profiles should be thoroughly assessed at the preclinical stage if the foreign nature of an expressed fusion or chimera protein may prove to be immunogenic, and also if aberrant expression of the transgene is known or suspected to induce toxicity.²² Due to the characteristics of GFP and its effects, these considerations are particularly salient with regard to rAAV2-shmTOR-GFP.

Derived from the *Aequorea victoria* jellyfish,²⁰ GFP has been often linked to cytotoxicity, and cell death is a general effect associated with GFP expression.^{23,24} Compared to YFP (yellow fluorescent protein) and CFP, other fluorescent reporter genes, GFP was found to have a special toxicity. As a result, GFP is unable to be propagated as stable cell lines, which is possible with both YFP and CFP, with this toxicity observed independent of transfection.²⁴ With GFP-transfected cells exhibiting morphological changes associated with apoptosis as well as elevated levels of CPP32,²³ an apoptosis indicator,²⁵ it is possible that this is the mechanism by which cell death occurs.²³ A similar effect was observed *in vivo*, as the laser-induced CNV mouse model retinas treated with rAAV2-shCon-GFP had slightly elevated levels of TUNEL-positive cells compared to the mock-treated reference group. Furthermore, both SD-containing virus vectors exhibited decreased numbers of apoptotic cells compared to their GFP-expressing counterparts. While our results may not be especially significant statistically, this may be due to the relatively short time frame, with sacrifice coming 8 days post-intravitreal injection. If GFP had been able to be expressed for a longer period of time, its cytotoxic effects may have proved to be far more dramatic.

GFP expression has also been associated with the generation of free radicals,^{20,23,26} to the point where such cells may be considered to always be under oxidative stress.²⁷ As such, further pursuing the mTOR-inhibiting shRNA as a human gene therapeutic for wet AMD requires the removal of the GFP expression cassette. In addition to cytotoxic concerns, a portion of GFP has been found to serve as a natural epitope of MHC class I molecules.²⁸ This was confirmed in rhesus macaques, wherein GFP elicited a relatively vigorous cytotoxic T lymphocyte response, exclusively through CD8⁺ lymphocytes.²⁹ Furthermore, GFP inhibits polyubiquitination, thereby reducing nuclear factor κ B (NF- κ B)- and JNK-signaling pathway activation, among other disruptions of cellular processes.³⁰

Simply excising GFP from the virus vector, though, would be inappropriate due to the specifics of AAV production and activity. The inclusion of a SD is necessary to maintain proper genome size and ensure

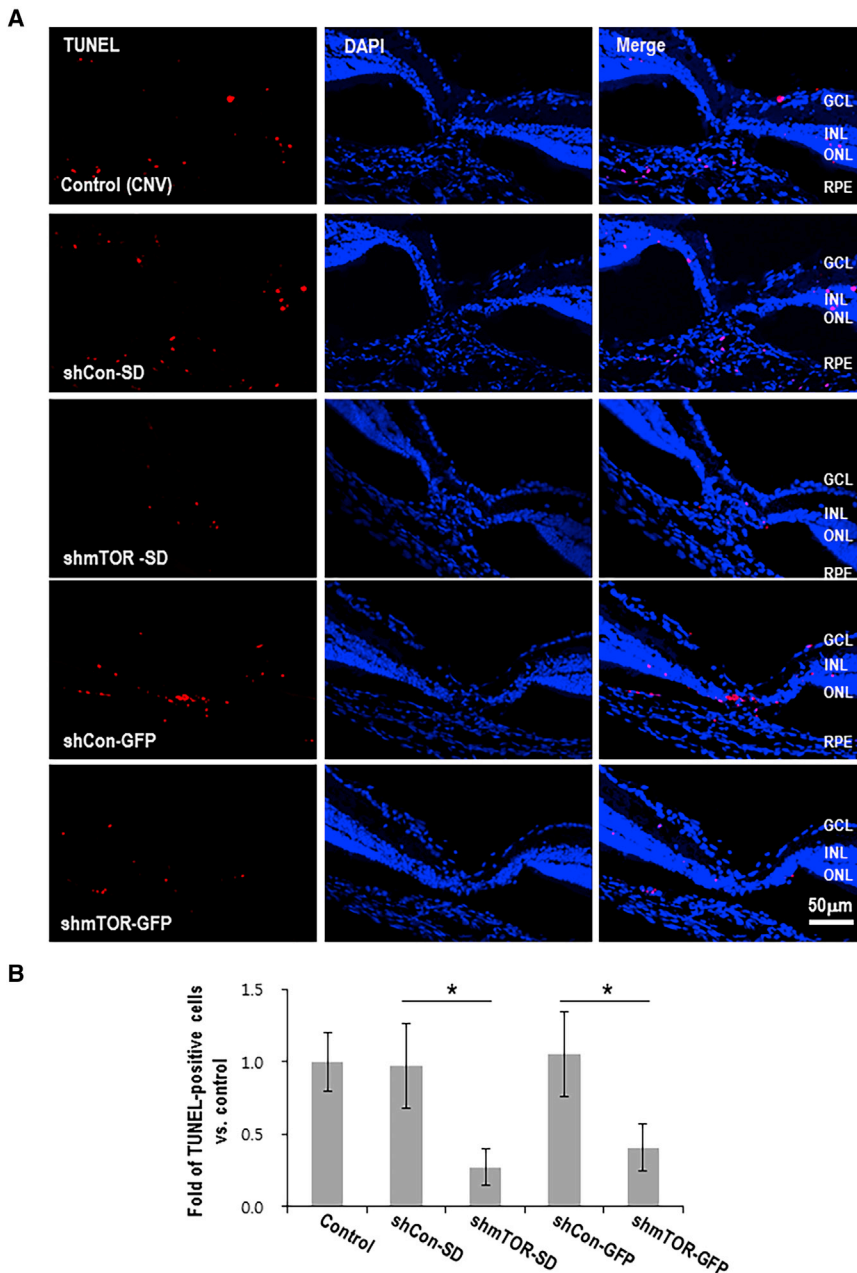


Figure 5. Anti-apoptotic Effect of rAAV2-shmTOR-SD, as Determined by TUNEL Assay

TUNEL-positive cells were observed in retinal sections of mock-treated mice and mice treated with virus vectors containing control shRNA. Significantly fewer apoptotic cells were detected in the retinas of mice treated with rAAV2-shmTOR-SD and rAAV2-shmTOR-GFP (A), showing that the mTOR shRNA has anti-apoptotic activity, with the results then quantified (B) ($n = 3$).

An additional complication is that rAAV2-shmTOR-SD utilizes a self-complementary AAV, which halves the capacity of the delivery vehicle,^{33,34} thereby reducing the size limit of a suitable prospective SD. Therefore, the much larger SDs used in adenovirus research, based on the hypoxanthine-guanine phosphoribosyl-transferase gene or phage lambda, would be unsuitable for these purposes.³⁵ The latter is especially inappropriate due to base composition concerns, with phage lambda DNA having a GC content of approximately 57%. This is similar to that of wild-type adenoviruses (55%), whereas mammalian DNA generally has a GC content of 41%. This discrepancy is thought to be responsible for the poor performance of these stuffers in mammalian cell lines, which may result from an immune response initiated by the stuffer³⁵ that is linked to the xenogeneic origin of the GFP gene.

However, some SDs have been used in adeno-associated virus vectors, including one derived from the 3' UTR of the human UBE3A gene.³⁶ Taken between positions 994 and 2,740, its size (1.75 kb) ensures that the viral genome is not too large to affect packaging while not being too small to affect infectivity. As can be seen, replacing the GFP expression cassette with this stuffer did not reduce the ability of rAAV2-shmTOR-SD to address the symptoms of wet AMD, and, in fact, it was generally seen to mildly improve upon the performance of rAAV2-shmTOR-GFP. A microarray analysis additionally revealed no off-target effects resulting from use of the SD (data not shown). This confirmed the results of deep sequencing performed by Strobel and colleagues³⁶ showing that the SD was silent with respect to gene expression changes. While a detailed off-targeting study to confirm that the SD does not yield a gene product would not be inappropriate, this lies beyond the scope of this study.

As such, replacing the GFP expression cassette with a SD taken from the 3' UTR of the human UBE3A gene is a necessary step for

optimal packaging efficiency,³¹ yet much of the research performed thus far on the characterization of SDs has involved those inserted into adenovirus vectors, which have a much larger carrying capacity. The optimal size for rAAV2, including transcription factors and inverted terminal repeats, has been reported to be 4.1–4.9 kb. Significantly larger viral genomes result in improper packaging, whereas virions resulting from smaller vectors are less infectious.³² Controlling TP:IP (total particle-to-infectious particle) ratios in the production of gene therapy virus vectors is thus crucial, as variations to this value make it difficult to properly perform quality control functions.

developing rAAV2-shmTOR-SD as a potential gene therapeutic against wet AMD. Having thus verified its mTOR-inhibiting ability *in vitro* and its effectiveness in reducing CNV in a laser-induced mouse model, where it exhibited anti-angiogenic and anti-apoptotic properties, the future plans for this virus vector include additional preclinical studies. These include long-term efficacy and safety studies, as well as ensuring there are no neutralizing antibody effects from the use of the rAAV delivery vehicle, all of which have already begun. The latter studies are necessary because immune responses may decrease transduction efficiency, resulting in diminished treatment efficacy, and this is specifically noted in the FDA's draft guidance on human gene therapy for retinal disorders.

While the success of Luxturna has shown that rAAV2 is a suitable vehicle for human gene therapeutics, its subretinal delivery has the advantage of bypassing the immune surveillance of the retina.³⁷ On the other hand, while the intravitreal administration of rAAV2-shmTOR-SD is more convenient for patients and does not require the general anesthesia and vitrectomy associated³⁸ with subretinal delivery, a comprehensive neutralizing antibody study is pertinent and necessary. Nonetheless, rAAV2-shmTOR-SD shows promise as a potential gene therapeutic versus wet AMD, for which the substitution of GFP with a SD is a prerequisite.

MATERIALS AND METHODS

Preparation of rAAV2-shmTOR-SD

pAAV-shmTOR-GFP was prepared as previously described⁷ and digested with ClaI and XhoI to remove the GFP expression cassette (CMV promoter [pCMV], GFP, and polyadenylation signal) and the 3' inverted terminal repeat (ITR). The human UBE3A gene fragment (accession number AH006486.2, position 994–2,740) attached to a 3' ITR flanked by EcoRI and XhoI restriction enzyme sites was obtained from GenScript (Nanjing, China). A linker oligonucleotide flanked with ClaI and EcoRI digestion sites was synthesized by Macrogen (Seoul, Korea). These fragments were ligated together to form the pAAV-shmTOR-SD construct, which was then used to produce rAAV2-shmTOR-SD. pAAV-shCon-SD was produced from pAAV-shCon-GFP in an analogous manner. All virus vectors used in this study were supplied by Cdmogen (Cheongju, Korea).

rAAV2-shmTOR-SD Characterization

Total RNA was prepared from ARPE-19 cells using TRIzol reagent (Invitrogen, Carlsbad, CA, USA), followed by the reverse transcription of RNA (2 mg) to cDNA using Superscript III (Invitrogen), and mRNA levels were analyzed using a SYBR Green kit (Invitrogen). Amplification was performed using primers specific to mTOR (forward, 5'-CCA CTGTGCCAGAATCCATC-3'; reverse, 5'-GAGAAATCCCCGACCA GTGAG-3') and β -actin (forward, 5'-TGAAGATCAAGATCATT GCTC-3'; reverse, 5'-TGCTTGCTGATCCACATCTG-3').

For western blots, ARPE-19 cells were treated with the virus vectors at 700 MOI and then lysed after 48 h. Retinal tissue from the mouse models was set aside prior to whole-mount and frozen section preparations, treated with 0.1 mL tissue grinders (Wheaton, Millville, NJ,

USA), and samples were prepared using M-PER Mammalian Protein Extraction Reagent (Thermo Fisher Scientific, Waltham, MA, USA), according to the manufacturer's instructions. SDS-polyacrylamide gels were used to resolve the proteins isolated from ARPE-19 cells or mouse retinal tissue, which were then transferred onto polyvinylidene fluoride membranes. Primary antibodies for mTOR, GFP, and β -actin were obtained from Cell Signaling Technology (2983; Danvers, MA, USA), Invitrogen (332600), and Sigma-Aldrich (A5441; St. Louis, MO, USA), respectively.

Animal Care

The 8-week-old male C57BL/6 mice were sourced from The Orient Bio (Sungnam, Korea) for this study. All animal care and experiments followed guidelines set forth in the Association for Research in Vision and Ophthalmology Resolution on the Use of Animals in Ophthalmic and Vision Research, and they were overseen by the Institutional Animal Care and Use Committee of Soonchunhyang University Hospital Bucheon.

Laser-Induced CNV

Prior to laser photocoagulation, the mice were anesthetized via intraperitoneal injection of a mixture of Zoletil (40 mg/kg zolazepam and tiletamine) from Virbac (Carros Cedex, France) and Rompun (5 mg/kg xylazine) from Bayer Healthcare (Leverkusen, Germany), and their pupils were dilated using Mydrin-P (0.5% tropicamide and 2.5% phenylephrine) sourced from Santen (Osaka, Japan). A 532-nm neodymiumdoped yttrium aluminum garnet PASCAL diode ophthalmic laser system (Topcon Medical Laser Systems, Santa Clara, CA, USA) was used for laser photocoagulation (200- μ m spot size, 0.02-s duration, 100 mW), wherein five or six laser spots were applied around the optic nerve of the right eye only. Gaseous bubble formation at the laser spot indicated the rupturing of Bruch's membrane.

Intravitreal Injections

At 5 days post-laser photocoagulation, the mice were placed under anesthesia and their pupils were dilated. 35G blunt needles (NF35BL-2; World Precision Instruments, Sarasota, FL, USA) were used to intravitreally inject 1 μ L virus vector at a concentration of 5×10^{10} viral genomes (vg)/mL into the right eyes only. Mock-treated animals were not subjected to intravitreal injections after the induction of CNV.

FFA

A Heidelberg Retina Angiograph 2 scanning laser ophthalmoscope (Heidelberg Engineering; Heidelberg, Germany) was used 13 days post-laser photocoagulation to observe the retinas of the CNV mouse model via FFA, as previously described.³⁹ After anesthetization and pupil dilation, 0.1 mL Fluorescite (2% fluorescein sodium solution) from Alcon Laboratory (Fort Worth, TX, USA) was injected intraperitoneally. FFA images were captured 3–5 min thereafter.

Tissue Preparation

The mice were deeply anesthetized using an intraperitoneally injected 4:1 mixture of zolazepam and tiletamine (80 mg/kg) and xylazine (10 mg/kg), followed by intracardial perfusion with 0.1 M PBS

(pH 7.4) containing 150 U/mL heparin and infusion with 4% paraformaldehyde (PFA) in 0.1 M phosphate buffer (PB). The eyeballs were enucleated for RPE-choroid whole mounts. The anterior segments, including the cornea and lens, were additionally removed to generate eyecups for frozen transverse retinal section samples. Eyecups were fixed in 4% PFA in 0.1 M PB (pH 7.4) for 2 h, transferred to 30% sucrose in PBS overnight, and embedded in Tissue-Tek, an optimal cutting temperature compound (Miles Scientific, Naperville, IL, USA), before preparing 10- μ m-thick sectioned samples.

Immunohistochemistry and TUNEL Assay

To immunostain whole mounts, RPE-choroid tissues were incubated overnight at 4°C with anti-GFP (ab6556; Abcam, San Francisco, CA, USA), anti-mTOR (AF15371; R&D Systems, Minneapolis, MN, USA), or mouse anti-CD31 (550274; BD Pharmingen, San Diego, CA, USA) diluted 1:200 in PBS containing 1% Triton-X (PBST; Sigma-Aldrich). This was followed by three washes in PBST for 10 min apiece and incubation with AlexaFluor 532-conjugated goat anti-mouse (A21270; Thermo Fisher Scientific) for 2 h at room temperature. To perform the TUNEL assay, the manufacturer's protocol (12156792910, Roche, Indianapolis, IN, USA) was followed for the retinal section samples, washed in PBST three times for 10 min apiece, and then stained with DAPI (D9542; Sigma-Aldrich) to visualize cell nuclei. The whole mounts and retinal sections were examined with an LSM 700 fluorescence confocal microscope (Carl Zeiss, Jena, Germany), and images were captured using ImageJ software (NIH, Bethesda, MD, USA).

Statistical Analysis

One-way ANOVA testing was used for statistical analysis and significant differences were determined at $p < 0.05$, $p < 0.01$, or $p < 0.001$. Boxplot graphs were used to visualize the data and include significance and mean \pm SEM values.

AUTHOR CONTRIBUTIONS

Conceptualization, H.L. and T.K.P.; Methodology, H.L., T.K.P., S.H.S.L., H.C., H.J.K., S.K.N., S.J.J., J.-S.C., J.K., H.-N.W., K.P., and J.Y.L.; Investigation, H.L., T.K.P., S.H.S.L., H.C., H.J.K., S.K.N., S.J.J., J.-S.C., J.K., H.-N.W., K.P., and J.Y.L.; Writing – Original Draft, H.L., S.H.S.L., and T.K.P.; Writing – Review & Editing, H.L., S.H.S.L., T.K.P., H.-N.W., K.P., and J.Y.L.

CONFLICTS OF INTEREST

The authors declare no competing interests.

ACKNOWLEDGMENTS

This work was supported by CuroGene Life Sciences Co., Ltd. and by grants from the Basic Science Research Program through the National Research Foundation of Korea (NRF-2017R1A2B4012769, 2017, to H.L.); the Asan Institute for Life Sciences, Asan Medical Center (2019-287 to H.L.); and the Korea Health Technology R&D Project through the Korea Health Industry Development Institute (KHIDI), funded by the Ministry of Health & Welfare (grant H17C0966 to

T.K.P.), Republic of Korea. For her proofreading and editing, we would also like to thank Paula Khim.

REFERENCES

- Wong, W.L., Su, X., Li, X., Cheung, C.M.G., Klein, R., Cheng, C.Y., and Wong, T.Y. (2014). Global prevalence of age-related macular degeneration and disease burden projection for 2020 and 2040: a systematic review and meta-analysis. *Lancet Glob. Health* 2, e106–e116.
- Nowak, J.Z. (2006). Age-related macular degeneration (AMD): pathogenesis and therapy. *Pharmacol. Rep.* 58, 353–363.
- Stewart, M.W. (2018). Extended duration vascular endothelial growth factor inhibition in the eye: failures, successes, and future possibilities. *Pharmaceutics* 10, E21.
- Singer, M.A., Awh, C.C., Sadda, S., Freeman, W.R., Antoszyk, A.N., Wong, P., and Tuomi, L. (2012). HORIZON: an open-label extension trial of ranibizumab for choroidal neovascularization secondary to age-related macular degeneration. *Ophthalmology* 119, 1175–1183.
- Nishijima, K., Ng, Y.S., Zhong, L., Bradley, J., Schubert, W., Jo, N., Akita, J., Samuelsson, S.J., Robinson, G.S., Adamis, A.P., and Shima, D.T. (2007). Vascular endothelial growth factor-A is a survival factor for retinal neurons and a critical neuroprotectant during the adaptive response to ischemic injury. *Am. J. Pathol.* 171, 53–67.
- Saint-Geniez, M., Maharaj, A.S.R., Walshe, T.E., Tucker, B.A., Sekiyama, E., Kurihara, T., Darland, D.C., Young, M.J., and D'Amore, P.A. (2008). Endogenous VEGF is required for visual function: evidence for a survival role on müller cells and photoreceptors. *PLoS ONE* 3, e3554.
- Park, T.K., Lee, S.H., Choi, J.S., Nah, S.K., Kim, H.J., Park, H.Y., Lee, H., Lee, S.H.S., and Park, K. (2017). Adeno-associated viral vector-mediated mTOR inhibition by short hairpin RNA suppresses laser-induced choroidal neovascularization. *Mol. Ther. Nucleic Acids* 8, 26–35.
- Laplante, M., and Sabatini, D.M. (2012). mTOR signaling in growth control and disease. *Cell* 149, 274–293.
- Liegl, R., Koenig, S., Siedlecki, J., Haritoglou, C., Kampik, A., and Kernt, M. (2014). Temsirolimus inhibits proliferation and migration in retinal pigment epithelial and endothelial cells via mTOR inhibition and decreases VEGF and PDGF expression. *PLoS ONE* 9, e88203.
- Nakahara, T., Morita, A., Yagasaki, R., Mori, A., and Sakamoto, K. (2017). Mammalian target of rapamycin (mTOR) as a potential therapeutic target in pathological ocular angiogenesis. *Biol. Pharm. Bull.* 40, 2045–2049.
- Stahl, A., Paschek, L., Martin, G., Gross, N.J., Feltgen, N., Hansen, L.L., and Agostini, H.T. (2008). Rapamycin reduces VEGF expression in retinal pigment epithelium (RPE) and inhibits RPE-induced sprouting angiogenesis in vitro. *FEBS Lett.* 582, 3097–3102.
- Dejneka, N.S., Kuroki, A.M., Fosnot, J., Tang, W., Tolentino, M.J., and Bennett, J. (2004). Systemic rapamycin inhibits retinal and choroidal neovascularization in mice. *Mol. Vis.* 10, 964–972.
- Saxton, R.A., and Sabatini, D.M. (2017). mTOR signaling in growth, metabolism, and disease. *Cell* 168, 960–976.
- Lee, H.S., Ahn, J., Jun, E.J., Yang, S., Joo, C.H., Kim, Y.K., and Lee, H. (2009). A novel program to design siRNAs simultaneously effective to highly variable virus genomes. *Biochem. Biophys. Res. Commun.* 384, 431–435.
- Ahn, J., Woo, H.N., Ko, A., Khim, M., Kim, C., Park, N.H., Song, H.Y., Kim, S.W., and Lee, H. (2012). Multispecies-compatible antitumor effects of a cross-species small-interfering RNA against mammalian target of rapamycin. *Cell. Mol. Life Sci.* 69, 3147–3158.
- Park, K., Kim, W.J., Cho, Y.H., Lee, Y.I., Lee, H., Jeong, S., Cho, E.S., Chang, S.I., Moon, S.K., Kang, B.S., et al. (2008). Cancer gene therapy using adeno-associated virus vectors. *Front. Biosci.* 13, 2653–2659.
- Ameri, H. (2018). Prospect of retinal gene therapy following commercialization of voretigene neparvovec-rzyl for retinal dystrophy mediated by RPE65 mutation. *J. Curr. Ophthalmol.* 30, 1–2.
- Lai, C.M., Estcourt, M.J., Wikstrom, M., Himbeck, R.P., Barnett, N.L., Brankov, M., Tee, L.B., Dunlop, S.A., Degli-Esposti, M.A., and Rakoczy, E.P. (2009). rAAV.sFlt-1

- gene therapy achieves lasting reversal of retinal neovascularization in the absence of a strong immune response to the viral vector. *Invest. Ophthalmol. Vis. Sci.* 50, 4279–4287.
19. Lee, S.H., Kong, Y.J., Lyu, J., Lee, H., Park, K., and Park, T.K. (2015). Laser photocoagulation induces transduction of retinal pigment epithelial cells by intravitreally administered adeno-associated viral vectors. *Hum. Gene Ther. Methods* 26, 159–161.
 20. Ansari, A.M., Ahmed, A.K., Matsangos, A.E., Lay, F., Born, L.J., Marti, G., Harmon, J.W., and Sun, Z. (2016). Cellular GFP toxicity and immunogenicity: potential confounders in in vivo cell tracking experiments. *Stem Cell Rev.* 12, 553–559.
 21. Center for Biologics Evaluation and Research (2018). Human gene therapy for retinal disorders: draft guidance for industry. In US Food and Drug Administration. July 2018, FDA-2018-D-2236, <https://www.fda.gov/regulatory-information/search-fda-guidance-documents/human-gene-therapy-retinal-disorders>.
 22. Center for Biologics Evaluation and Research (2013). Preclinical assessment of investigational cellular and gene therapy products: guidance for industry. In US Food and Drug Administration. November 2013, FDA-2012-D-1038, <https://www.fda.gov/regulatory-information/search-fda-guidance-documents/preclinical-assessment-investigational-cellular-and-gene-therapy-products>.
 23. Liu, H.S., Jan, M.S., Chou, C.K., Chen, P.H., and Ke, N.J. (1999). Is green fluorescent protein toxic to the living cells? *Biochem. Biophys. Res. Commun.* 260, 712–717.
 24. Taghizadeh, R.R., and Sherley, J.L. (2008). CFP and YFP, but not GFP, provide stable fluorescent marking of rat hepatic adult stem cells. *J. Biomed. Biotechnol.* 2008, 453590.
 25. Woo, M., Hakem, R., Soengas, M.S., Duncan, G.S., Shahinian, A., Kägi, D., Hakem, A., McCurrach, M., Khoo, W., Kaufman, S.A., et al. (1998). Essential contribution of caspase 3/CPP32 to apoptosis and its associated nuclear changes. *Genes Dev.* 12, 806–819.
 26. Ganini, D., Leinisch, F., Kumar, A., Jiang, J., Tokar, E.J., Malone, C.C., Petrovich, R.M., and Mason, R.P. (2017). Fluorescent proteins such as eGFP lead to catalytic oxidative stress in cells. *Redox Biol.* 12, 462–468.
 27. Koike, M., Yutoku, Y., and Koike, A. (2012). Ku80 attenuates cytotoxicity induced by green fluorescent protein transduction independently of non-homologous end joining. *FEBS Open Bio* 3, 46–50.
 28. Gambotto, A., Dworacki, G., Cicinnati, V., Kenniston, T., Steitz, J., Tüting, T., Robbins, P.D., and DeLeo, A.B. (2000). Immunogenicity of enhanced green fluorescent protein (EGFP) in BALB/c mice: identification of an H2-K^d-restricted CTL epitope. *Gene Ther.* 7, 2036–2040.
 29. Rosenzweig, M., Connoles, M., Glickman, R., Yue, S.P.S., Noren, B., DeMaria, M., and Johnson, R.P. (2001). Induction of cytotoxic T lymphocyte and antibody responses to enhanced green fluorescent protein following transplantation of transduced CD34⁺ hematopoietic cells. *Blood* 97, 1951–1959.
 30. Baens, M., Noels, H., Broeckx, V., Hagens, S., Fevery, S., Billiau, A.D., Vankelecom, H., and Marynen, P. (2006). The dark side of EGFP: defective polyubiquitination. *PLoS ONE* 1, e54.
 31. Grimm, D., Pandey, K., and Kay, M.A. (2005). Adeno-associated virus vectors for short hairpin RNA expression. *Methods Enzymol.* 392, 381–405.
 32. Dong, J.Y., Fan, P.D., and Frizzell, R.A. (1996). Quantitative analysis of the packaging capacity of recombinant adeno-associated virus. *Hum. Gene Ther.* 7, 2101–2112.
 33. Grieger, J.C., and Samulski, R.J. (2012). Adeno-associated virus vectorology, manufacturing, and clinical applications. *Methods Enzymol.* 507, 229–254.
 34. Wu, J., Zhao, W., Zhong, L., Han, Z., Li, B., Ma, W., Weigel-Kelley, K.A., Warrington, K.H., and Srivastava, A. (2007). Self-complementary recombinant adeno-associated viral vectors: packaging capacity and the role of rep proteins in vector purity. *Hum. Gene Ther.* 18, 171–182.
 35. Parks, R.J., Bramson, J.L., Wan, Y., Addison, C.L., and Graham, F.L. (1999). Effects of stuffer DNA on transgene expression from helper-dependent adenovirus vectors. *J. Virol.* 73, 8027–8034.
 36. Strobel, B., Duechs, M.J., Schmid, R., Stierstorfer, B.E., Bucher, H., Quast, K., Stiller, D., Hildebrandt, T., Mennerich, D., Gantner, F., et al. (2015). Modeling pulmonary disease pathways using recombinant adeno-associated virus 6.2. *Am. J. Respir. Cell Mol. Biol.* 53, 291–302.
 37. Constable, I.J., Lai, C.M., Magno, A.L., French, M.A., Barone, S.B., Schwartz, S.D., Blumenkranz, M.S., Degli-Esposti, M.A., and Rakoczy, E.P. (2017). Gene therapy in neovascular age-related macular degeneration: three-year follow-up of a phase 1 randomized dose escalation trial. *Am. J. Ophthalmol.* 177, 150–158.
 38. Davis-Smyth, T., Chen, H., Park, J., Presta, L.G., and Ferrara, N. (1996). The second immunoglobulin-like domain of the VEGF tyrosine kinase receptor Flt-1 determines ligand binding and may initiate a signal transduction cascade. *EMBO J.* 15, 4919–4927.
 39. Han, J.W., Lyu, J., Park, Y.J., Jang, S.Y., and Park, T.K. (2015). *Wnt1*/β-catenin signaling mediates regeneration of retinal pigment epithelium after laser photocoagulation in mouse eye. *Invest. Ophthalmol. Vis. Sci.* 56, 8314–8324.